ISSN:0975-3583,0976-2833 VOL12,ISSUE04,2021

Coronary Artery Vulnerable Plaque Detection And Characterization: What Do Cardiologists Need To Know?

Noha Yahia Ebaid[1], Dalia Nabil Khalifa[2,] Ahmad Sabry Ragheb[3], Magdy Mohamad Abdelsamie[4],EssamElsayed Tharwat[5], and Ahmed Mohamed Alsowey[6]

[1,2,3,5,6]Department of Radiology, Faculty of Medicine, ZagazigUniversity, Egypt.; e-mail@e-mail.com

[4]Department of Cardiology, Faculty of Medicine, ZagazigUnivesity, Egypt.; e-mail@e-mail.com

Email: nohayahiaradio@gmail.com

Abstract:

Acute coronary syndrome is often precipitated by a sudden thrombosis induced by the rupture or erosion of an atherosclerotic plaque. In individuals with acute chest pain, culprit lesions' non-invasive detection has the ability to improve non-invasive risk classification. Coronary computed tomography angiography [CCTA] detects luminal stenosis and visualizes atheromatous mural changes [coronary plaques]. A higher risk of acute cardiovascular events is seen in individuals having a large plaque volume, positive remodeling, napkin-ring sign, spotty calcification, and low CT attenuation. Coronary CTA has shown to be a promising method for determining coronary lesions' functional significance via the use of rest/dynamic myocardial CT perfusion and/or CT-derived fractional flow reserve [FFR-CT]. Other invasive procedures as intravascular ultrasound and optical coherence topography gain important insights but are limited to high-risk patients.

Key Words:

Coronary;Plaque; Computed Tomography; Characterization; Napkin ring.

1. INTRODUCTION

Atherosclerosis is an arterial wall degenerative process that mostly affects large and medium-sized systemic arteries. Angina pectoris and other clinical ischemic symptoms are frequent as a result of a coronary plaque that forms flow-limiting stenosis, therefore decreasing the perfusion of the tissues [1]. If this clinical state persists, the atherosclerotic plaques are considered stable fibrotic morphology lesions [2].

Unexpected incidents such as stroke and myocardial infarction happen due to a sudden shift in clinical dysfunction [3]. A sudden rupture and subsequent thrombosis of an atherosclerotic plaque is the primary reason for the transition from asymptomatic to symptomatic illness [4].

These "vulnerable" lesions may be non-obstructive as well [5]. A "vulnerable plaque" is a non-obstructive, silent lesion of the coronary that progresses to become obstructive and symptomatic [6], and it leads to the majority of acute coronary conditions [7]. Also, vulnerable plaques are prone to thrombosis and can develop a culprit lesion quickly. The following major and minor criteria were used to determine plaque vulnerability degree: a thin cap [100 m] with a large lipid core [greater than 50% of the total volume of the plaque], superficial platelet aggregation or endothelial denudation, active inflammation, and stenosis [greater than 90%] are considered as major criteria. A superficial calcified nodule, endothelial dysfunction, intraplaque hemorrhage[IPH], and plaque color are all considered minor criteria [8].

2. PLAQUE COMPOSITION IN ACUTE CORONARY SYNDROME

2.1. Presentation

The three types of the acute coronary syndrome are unstable angina, ST-segment elevation myocardial infarction, and non-ST-segment elevation myocardial infarction [9]. The majority of ACS events [two-thirds] are caused by abrupt luminal thrombosis or erosion [one-third][10-12].

A ruptured plaque consists of a big necrotic core [often greater than 30% of the plaque area in two-thirds] and a luminal thrombus linked to the necrotic core via a gap in a thin [65 m] burst fibrous cap [10,13]. A plaque with less than 3 mm core diameter, an area less than 1.0 mm2, a cap thickness less than 150 m, and a core percentage less than 10% has a minimal rupture risk. [13,14].

There are fewer inflammatory cells and nonocclusive thrombi in erosive plaques than in plaque ruptures [12].

2.2. Associated Findings in Plaque Instability

Since most clinical CT scanners have a poor spatial resolution, detecting a thin fibrous cap is impossible; thus, additional characteristics must be utilized to categorize plaques at increased rupture risk. [15]. In positive remodeling early stages, plaques become more vulnerable to break up, and their stability is determined by necrotic core thickness rather than area [15]. Positive remodeling, which is characteristic of plaques with large necrotic cores, TCFA, and bleeding, indicates plaque instability [15].

3. IMAGING TECHNIQUES FOR PLAQUE DETECTION AND CHARACTERIZATION

ISSN:0975-3583,0976-2833 VOL12,ISSUE04,2021

3.1. Invasive techniques :

3.1.1 Intravascularultrasound[IVUS]

An ultrasound device is attached to the catheter's tip [16]. The beam will be manually guided for single-element catheters, while for arrays, the beam will be electronically steered. [17]. Rotation devices can generate images with a resolution of 100 to 150 meters [18]. In general, phased array catheters are more flexible and simpler to set up [19]. These catheters may be inserted through the coronary arteries through the groin, then through the aorta, providing arterial, vessel wall, and atherosclerosis tomographic images [17].
Calculations of lumens are based on the contact between the lumen and the intima leading edge [20]. Gray-scale IVUS helps in determining the atherosclerotic plaque severity, size, and distribution. Additionally, it may be beneficial in cross-sectional area calculation. [21]. Lipid-laden lesions produce low-intensity or "soft" echoes, whereas lesions composed of fibrous or calcified material are quite echogenic. [Fig 1.]. Based on the acoustic signal, IVUS Greyscale is capable of identifying four distinct plaque types [22].

(A) 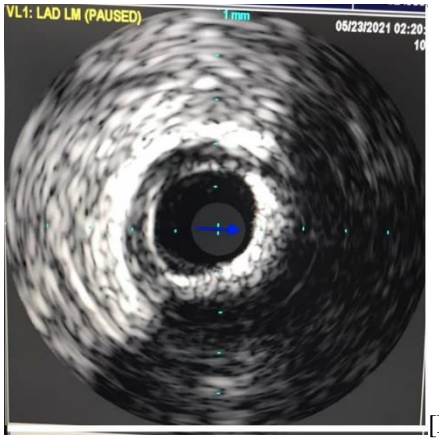

[B] 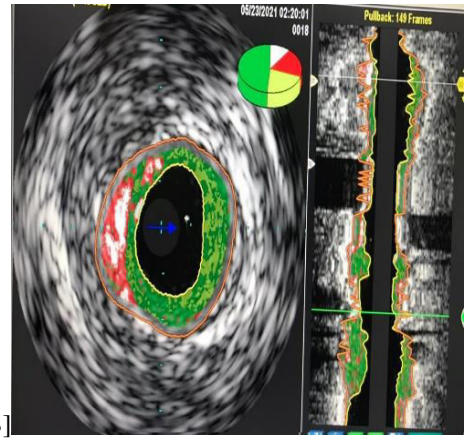

Figure. 1. [a]Gray-scale by IVUS shows heavily calcified plaque from 1 to 7 o'clock.**[b]**Image by IVUS-VH in different patients shows different components of plaque. Plaque composition: Red: necrotic core, Dark green: fibrous, Light green: fibro-fatty, White: calcified plaque.

Due to the fact that the greatest resolution available for IVUS is 100 m, finding a thin cap [defined as 65 m] proved challenging. Greyscale IVUS may be insufficient for identifying lipid-rich and hence unstable plaques. However, an eccentric atheroma with a large plaque load is more prone to rupture, as shown by a shallow echo lucent zone identified by Greyscale IVUS. [23].
While Grayscale IVUS has enhanced the percutaneous coronary intervention [PCI] field, its inter-and intra-observer subjectivity and its axial resolution restrict its capacity to identify plaque subtypes. VHIVUS [virtual histology intravascular ultrasound] enables real-time plaque subtype categorization. This method is identical to the classic Greyscale method in terms of equipment and ultrasonic technology, but it performs spectrum analysis on the raw backscattered data. Radiofrequency data are transformed into a power spectrum graph that plots the backscattered US signal amplitude versus frequency via VHIVUS and by using autoregressive modelling [21].
Using statistical classification trees and a combination of spectrum characteristics, the radiofrequency data were classified into four types of plaque: fibrous, fibro-fatty, necrotic heart, and dense calcium plaque. [24].
A lesion that satisfies at least three of the following criteria is defined as an IVUS-derived thin-cap fibroatheroma [IDTCFA]: 1] tiny luminal region [4.0 mm2], 2] a high plaque pressure [70%], and 3] the existence of a thin-cap fibroatheroma. The absence of IDTCFA, on the other hand, was linked with relative stability, and lesions with a less than 10% necrotic core had a low chance three years later of triggering a major adverse cardiac event [MACE] [25].
Endovascular ultrasound elastography [IVUSe] is used to assess the mechanical characteristics of vascular tissues. The strain values in lipid-rich regions are substantially higher than in fibrous-rich regions. As a result, an atheroma with a thin fibrous cap is more susceptible to circumferential stress, resulting in an increase in strain on the elastogram[26].

3.1.2. Optical Coherence Tomography [OCT]

OCT is intracoronary imaging comparable to IVUS. Instead of ultrasound, it employs near-infrared radiation. It boasts a tenfold increase in image resolution [10 to 20 m] and a tenfold increase in tissue contrast over

ISSN:0975-3583,0976-2833 VOL12,ISSUE04,2021

traditional IVUS. Three layers of the coronary artery wall may be identified using OCT because of the improved intraluminal image quality, which are a signal-rich layer closest to the lumen known as intima, a signal-poor intermediate layer media as media, and a signal-rich layer surrounding the media as adventitia [27].
OCT may detect fibrous cap thickness, macrophage invasion, lipid content, calcium content, plaque rupture, thrombi, and vascular remodeling, among other plaque characteristics [28].

3.1.3. Near-infrared spectroscopy [NIRS]
The lipid content of plaques can be imaged using NIRS [29].
3.2. Non-invasive techniques:

3.2.1 Magnetic resonance imaging [MRI]
Magnetic resonance imaging [MRI] is a non-invasive imaging technique that can be utilized to characterize "vulnerable" high-risk plaques and determine the overall level of atherosclerotic carotid pressure in patients with symptoms. To identify the plaques anatomy and composition, T1-weighted, T2-weighted, and proton density-weighted imaging can be used. Multiple MR sequences, either with or without bright-blood flow suppression, may assist in detecting the vascular lesions primary components, such as the lipid-rich necrotic core [LRNC], the neovasculature, the IPH, the fibrous cap, and evidence of inflammation of the vascular wall [30].
In patients with mild to moderate stenosis, the thin/ruptured fibrous cap and a lipid-rich necrotic core were related to symptoms, whereas in those having severe stenosis, only the presence of ulceration at MR was found symptomatic [31]. In individuals with 50%–79% carotid stenosis, plaques with a thinned or ruptured fibrous cap, IPH, a broad lipid necrotic heart, and a maximum wall thickness were associated with a higher cerebrovascular events incidence [32].
Although approved sequences and specialized coils for MRI imaging of the vulnerable plaques and carotid arteries are available, cardiac and respiratory movements currently limit the efficacy of coronary tree imaging[33].

3.2.2. Nuclear imaging
In atherosclerosis imaging, nuclear methods can be used due to the fact that inside the plaque, the radiotracer may colocalize with a target receptor or cell, demonstrating its functional characteristics via gamma-ray emission. These features may be used to identify inflammatory and rupture-prone lesions non-invasively. The nuclear imaging key benefit is its high sensitivity that enables identifying nanomolar targets with a minimal tracer dose [8].

3.2.3 Computed tomography [CT]
The new CT scanner's excellent temporal and spatial resolution enables precise large and medium-sized arteries anatomical delineation, making it the most precise clinical equipment available for non-invasive coronary angiography [34].
It may also be utilized to visualize coronary artery disease early stages. Non-contrast CT is capable of detecting and quantifying coronary calcium, a proxy marker for coronary atherosclerotic plaque presence and volume, enabling us to stratify asymptomatic individuals [35].
Coronary calcium assessments through CT may be beneficial in individuals at a moderate risk of coronary artery disease [CAD] based on risk factors prior to assessment. It can also be useful when determining whether or not to begin lipid-lowering therapy. The calcified structures' high CT attenuation permits plaque composition evaluation quantitatively and visually by subdividing coronary lesions into calcified, non-calcified, and mixed plaques [Fig. 2a-c]. Surprisingly, individuals with ACS exhibited a greater incidence of non-calcified and mixed plaques in the culprit lesions, whereas typical calcified lesions were more in those having stable angina. Diffuse intraplaque calcification may not be linked to vulnerability, according to this data. Spotty calcified deposits along a 90° arc were detected in patients with AMI in particular [36].

(A)

ISSN:0975-3583,0976-2833 VOL12,ISSUE04,2021

(B)

Figure. 2. CT images of non-calcified plaque, mixed plaque and calcified plaques **[a]**Example of mixed and non-calcified plaques MDCT curved multiplanar reconstruction of the left anterior descending artery [LAD] showed a mixed calcified plaque in the proximal segment [Curved arrow] and non-calcified plaque in the mid-segment associated with non-significant obstruction of the lumen [<50%][Straight arrow]. **[b]** Example of multiple spotty calcified plaques of left anterior descending [LAD][arrows] without significant luminal obstruction. **[c]**MDCT curved multiplanar reconstruction of the left anterior descending artery [LAD] showed calcified [curved arrow] and mixed [Straight arrow] plaques in the mid-segment of the LAD.Note the artifact of "blooming" due to partial volume averaging of dense calcium [which typically has an elevated atomic number]. The median of MDCT densities of the plaques at this level was 780 HU.

MDCT is a non-invasive standard criterion that appears to be promising and can be used in conjunction with invasive imaging modalities [35].

Thin-cap fibroatheromas [TCFAs] identified by IVUS are linked to lesions categorized as mixed on CT angiography [CTA] in ACS patients [37]. There is insufficient evidence to support a reliable categorization of non-calcified plaques as fibrous or lipid-rich on the basis of CT density measurements[38]. CTA can detect significant plaque and necrotic core sizes, as well as external vascular remodeling in susceptible plaques. In acute coronary events, positively remodeled lesions have patchy calcium deposits and encompass a large soft region [< 30 Hounsfield units][8].

The appearance of all three features in a plaque meant that the lesion was 95 % likely to be a culprit lesion [39].

Contrast enhancement, ring-like, around the coronary lesion has been proposed as a plaque fragility new sign. This imaging phenomenon may be due to large necrotic core isolation from the native vessel wall or fibrous contents [40,41]. Despite being insensitive, this sign was discovered to be the most strong MDCT characteristic linked with TCFA at the culprit location, having >95% specificity [40].

Future advances will enhance MDCT's ability to identify susceptible plaques, such as the utilization of multiple energy data sets, the reduction of plaque component attenuation overlap, and visualization of histological abnormalities that may be indicative of clinical susceptibility. Additionally, CT has shown

ISSN:0975-3583,0976-2833 VOL12,ISSUE04,2021

promising initial findings in the setting of intra-plaque inflammation molecular imaging utilizing tailored nanoparticle contrast agents such as N1177. [42].

4. THE TECHNIQUE OF CORONARY CT ANGIOGRAPHY AND PLAQUE CHARACTERIZATION

4.1. Data acquisition:

An MDCT scanner was used to obtain multi-detector computed tomography results. According to the protocol, images were obtained with 16 0.75 mm slice collimation, a 420 ms gantry rotation time, a 2.8 mm/rotation table feed, a 120 kV tube energy, and a 500 mAs effective tube current [43]. Contrast agent [80 milliliters, Iodhexodol 320 g/cm3] was administered intravenously at a rate of 4 ml/s. Metoprolol [5 mg] intravenously was given to all patients with a heart rate of 65 beats/min before the MDCT scan. Using an ECG-gated half-scan technique, the overlapping transaxial images were reconstructed with an image matrix of 512 512 pixels, a 1 mm slice thickness, and 0.5 mm increment, resulting in a temporal resolution of 210 ms at the center of rotation. The ECG was retrospectively gated during image reconstruction. To reduce motion artifacts, the reconstruction window location during the cardiac cycle was optimized on an individual basis. Around 80%–90% of arteries have an optimum diastolic window between 55%–65% of the RR interval, according to our experience. Three data sets were reconstructed on average for each patient [44].

4.2. MDCT image evaluation:

Using a modified 17-segment coronary artery model, each lesion was classified according to its location [45]. Readers were provided with the precise location of each lesion site of maximum luminal constriction as assessed by quantitative coronary angiography using anatomical landmarks [branches and ostia]. Original axial photographs, cross-sectional reconstructions [1-mm thickness], and multiplanar reconstructions perpendicular to the vessel centerline were taken at the maximal narrowing of the lumen and at reference sites proximal and distal to the lesion in order to assess the lesions. With a fixed setting [700 Hounsfield units [HU] window, 200 HU level], the images were initially presented at the site of maximal narrowing of the lumen [46].

4.3. Detection of coronary atherosclerotic plaque:

The atherosclerotic plaque was identified by examining the cross-sectional image at the maximal luminal constriction [Fig. 3]. Visual identification of non-calcified and calcified plaque in coronary arteries can be made. Any visible structure attributed to the coronary artery wall was identified as non-calcified plaque using computed tomography [CT] attenuation in at least two independent planes below the contrast-enhanced coronary lumen but above the surrounding connective tissue/epicardial fat [6].

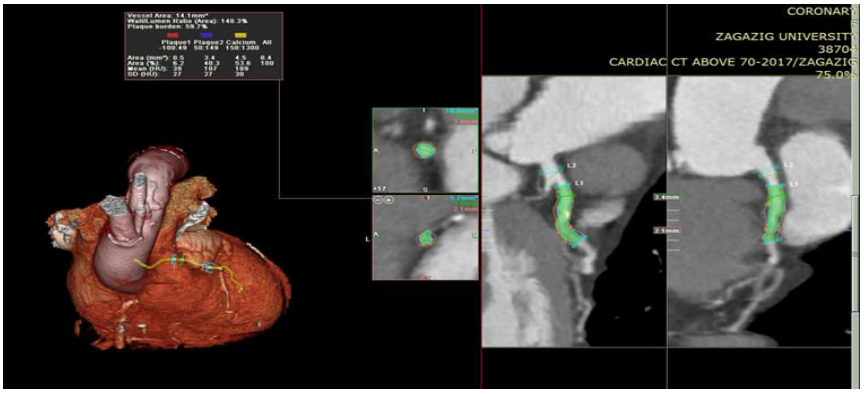

Figure. 3. Example of plaque characterization and quantification using a dedicated automated software tool of vitreaworkstation.

4.4. Degree of coronary stenosis:

To maximize sensitivity for calcified atherosclerotic plaque identification, any structure with a CT attenuation of 130 HU that could be seen independently of the contrast-enhanced coronary lumen was classified as calcified atherosclerotic plaque [47].

The stenosis degree was determined by the ratio of the luminal area at the maximum stenosis point to the mean luminal area at the proximal and distal reference sites [47].

ISSN:0975-3583,0976-2833 VOL12,ISSUE04,2021

Plaque area and coronary remodelling assessment:

az

5. CCTA PLAQUE CHARACTERIZATION:

5.1. Morphology:

5.1.1. Composition:

Coronary plaques can be categorized, depending on the calcium quantity in the lesion, as non-calcified, partly calcified, or calcified [48]. There was an important impact on mortality with partly calcified or calcified plaque [49].

5.1.2. Criteria of vulnerable plaque:

5.1.2.1.Low CT attenuation plaques

The CT distinction between plaques composed mostly of lipid-rich material and plaques composed primarily of fibrous material is beneficial for ACS prediction because lesions that result in ACS also have a wide necrotic lipid-rich core [50].

It was possible to distinguish between calcified plaque components and non-calcified plaque components [46]. However, classifying NCPs into lipid-rich and fibrous lesions using CT attenuation values [as assessed by HU] remains difficult. Some researchers have conducted comparisons between CCTA plaque assessments and the clinical reference standard IVUS and found that lipid-rich plaques have low CT attenuation on average [51].

NCPs with a high CT attenuation were correlated with fibrous tissue, whereas those with a low CT attenuation were correlated with necrotic core and fibrofatty tissue, as assessed by VH-IVUS. Within plaque styles, however, there is a lot of variation in CT values [52].

In spite of the fact that fibrous and lipid-rich plaques mean densities differ, the overlap of densities prevented NCPs from being reliably subclassified [51,52].

As a result, the accurate distinction between fibrous and lipid-rich lesions based only on CT attenuation is currently impossible [53].

Some of these limitations may be overcome by emerging automated plaque quantification software tools that incorporate scan-specific adaptive attenuation threshold settings, thereby enhancing the quantification of plaque components using CT numbers. [55,54].

Low plaque attenuation was identified as less than 30 HU [Fig. 4], and 88% of ruptured plaques had it, compared to 18% of stable lesions [56].

5.1.2.2 . Napkin-ring sign

A ruptured or TCFA plaque may be distinguished from a healthy plaque through a broad necrotic core cross-sectional area [>3.5 mm2][15]. In most plaques prone to rupture, the necrotic core is more than 1.0 mm^2. These values exceed the CCTA detection limit, enabling individual coronary plaques non-invasive risk assessment based on a massive necrotic heart presence or absence [57- 59].

The napkin-ring sign [NRS] refers to this distinct pattern of plaque attenuation [60]. The NRS is a qualitative plaque characteristic defined by the presence of two characteristics in a cross-section of a non-calcified plaque: a low-attenuation core zone that seems to be in contact with the lumen and a ring-like region with increasing attenuation surrounding this central region [60,61][Fig. 4].

NRS was observed in both non-contrast and contrast-enhanced ex vivo CT scans, indicating that the pattern is caused by contrast attenuation differences between the broad necrotic core [low CT attenuation in the center] and fibrous plaque tissue [ring-like higher attenuation][60].

NRS is quite accurate in detecting advanced coronary plaque and TCFA in CT [61]. A pattern-based plaque classification method has been created based on a comprehensive examination of plaque attenuation patterns. It categorizes non-calcified plaques as heterogeneous or homogeneous and heterogeneous plaques as non-NRS or NRS lesions. [61,62].

In TCFA plaques, the NRS was more common than in non-TCFA ones identified by OCT [58].

5.1.2.3. Positive remodeling

Because of the impact of positive remodeling, major luminal narrowing is not caused by rupturing-prone plaques. Positive remodeling refers to the compensatory vessel wall expansion at the atherosclerotic lesion site as the plaque size grows [Fig. 4], preserving the luminal region. [63].

The outer vessel wall and lumen dimension can be measured using CCTA [64,65, and 66]. The remodeling index is determined by dividing the cross-sectional vessel area at the maximum stenosis site by the average of the cross-sectional areas of the proximal and distal reference sections. [65,67].

On the basis of IVUS research, for the positive remodeling concept shown by CCTA, a remodeling index threshold of 1.1 has been suggested, but some researchers believe the cut-off point is 1.05 or higher [66, 67]. The remodeling index can now be easily quantified thanks to automated tools [54].

ISSN:0975-3583,0976-2833 VOL12,ISSUE04,2021

When comparing lesions with positive remodeling to lesions without positive remodeling on CCTA, they had a more necrotic heart, larger plaque load, and a greater TCFA prevalence as determined by VH-IVUS [68]. Additionally, on comparing TCFA lesions to non-TCFA lesions identified by OCT, the CT-derived remodeling index was greater [58].

Figure. 4. MDCT curved multiplanar reconstruction of the right coronary artery [RCA] showed non-calcified atherosclerotic plaque [arrow] with LAP, napkin-ring sign, and PR in the mid-segment on coronary CTA.

5.1.2.4. Spotty calcium in plaques

Coronary calcification as measured by CT is strongly linked to plaque burden and is associated with a poor clinical outcome [69].

While most acute plaque ruptures in people who die suddenly have some calcification on histopathology, about two-thirds of them had microcalcification only, which is undetectable on CT [63]. Spotty calcification is a CCTA term that refers to a tiny, thick [>130 HU] plaque segment surrounded by uncalcified plaque tissue. In CCTA, the typical cut-off for determining if a minor calcification is spotty is 3 mm. [Fig. 5][70,71].

Spotty calcifications have been classified as small [less than 1 mm], intermediate [1–3 mm], and massive [greater than 3 mm][72]. Furthermore, ACS culprit lesions are associated with spotty calcification [57,71].

Microcalcifications, which have been suggested to be a common characteristic of dysfunctional angina, could be detectable with more advancements in CT technology [73].

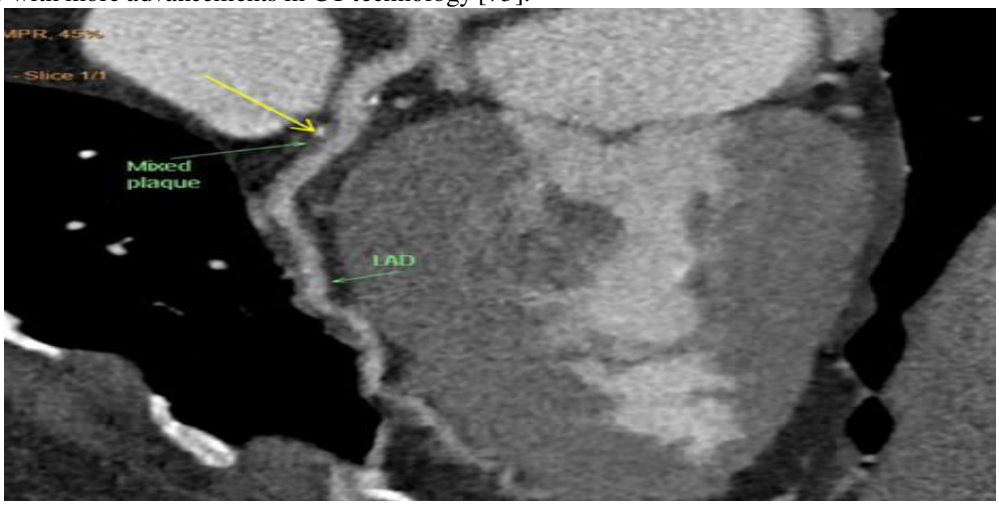

Figure. 5. MDCT curved multiplanar reconstruction of the left anterior descending artery [LAD] showed a mixed atherosclerotic plaque with spotty calcification in the proximal segment on coronary CTA [yellow arrow].

5.2. Functional characteristics:

Endothelial shear stress [ESS] and other hemodynamic variables are pathologically necessary for atherosclerotic plaque spatial localization and growth [63].

ISSN:0975-3583,0976-2833 VOL12,ISSUE04,2021

When applied to a standard CCTA dataset, CFD may be used to determine ESS-CT and FFR-CT coronary maps. [74,75].

5.2.1. ESS-CT:

The blood friction against the arterial wall endothelium produces a tangential force, which is known as ESS [76]. In low or turbulent flow, gene expression of the endothelial cell starts a proatherogenic cycle. [63].

Low ESS over time decreases nitric oxide intake, increases LDL uptake, causes local oxidative stress, and stimulates endothelial cell apoptosis, all of which contribute to the development of atherogenic endothelial phenotypes and high-risk lesions [77].

High shear stress at the plaque stenotic region can trigger pathophysiologic processes that cause plaque rupture [78].

The segments with a low ESS had a larger plaque area, necrotic core, and constrictive remodeling, whereas segments with a high ESS had excessive positive remodeling fibrous, fibrofatty tissue regression, and greater necrotic core indicating a shift to a more susceptible phenotype [79].

CCTA might be used to assess the ESS distribution in the major arteries and bifurcation areas [80].

5.2.2.FFR-CT:

At the time of the acute case, plaque rupture causes significant luminal narrowing [81,82]. Since there was a clear link between inflammatory cytokine activity and FFR, ischemia can play a role in plaque progression and destabilization [63]. Furthermore, an exploratory study revealed that unfavorable plaque characteristics seen by CCTA, positive remodeling, and low attenuation plaque were significant predictors of ischemia of myocardium in obstructive plaques [83].

FFR-CT aids in ischemia lesions diagnosis and will almost certainly enhance the sensitivity of CT for detecting high-risk lesions. Furthermore, without the need for external imaging, radiation, or medicine, FFR-CT may be acquired using CCTA. Additionally, from a single CCTA test, FFR-CT provides a three-vessel FFR, allowing FFR measurements along the coronary tree at any location [84].

The capacity to place a stent in a simulated environment and predict functional results based on changes in FFR is a novel use of CFD [85].

5.3.Parameters indicate the complexity of PCI:

Complex PCI procedures may involve the use of high-pressure balloons, buddy wire, kissing balloons, or rotablators. Before invasive diagnostics, pre-procedural lesion assessment by CCTA can offer significant extra information about the complexity of the lesion, allowing for early stratification of the most effective PCI approach. Procedure failure for CTO has been linked to lesion length >15 mm, target vessel tortuosity, and extreme calcification as measured by CCTA and unenhanced computed tomography [CT][86,87].

When lesions treated with complex PCI are in comparison with those with non-complex therapies, the median Agatston score, Hounsfield Units, and median local plaque volume are normally higher. On the other hand, PCI complexity had no statistically significant relationship with the degree of stenosis, plaque thickness, side branch involvement, or lesion shape. [89].

6. PLAQUE BURDEN

In cross-sectional studies, a big plaque volume was related to Acute Coronary Syndrome [ACS]. Quantifying non-calcified plaques [NCP] will aid in risk stratification and enhance CCTA predictive value for prospective cardiovascular events [90].

CT data sets with isotropic spatial resolution, in addition to the ability to describe tissue using CT attenuation, allows measuring the total coronary plaque burden and individual plaque components in a manner comparable to IVUS results [91,92]. Automated software approaches may now be used to quantify and characterize plaques. Automated plaque quantification is ideal because it improves CCTA plaque analysis. The automated coronary plaque quantification capability of CCTA has been verified effectively against greyscale IVUS and VH-IVUS. [54-64].

Due to the fact that the fragile plaques and ruptured culprit lesions are typically large in size when evaluated using histology or invasive imaging approaches, it is hypothesized that quantification of CCTA images has the potential to gradually improve the risk classification of patients over conventional CCTA readings. [50].

Multiple composite plaque burden scores, as well as CONFIRM and Learman scores, are produced using coronary CTA [93].

7. PREDICTORS OF FINDINGS FOR PRIMARY OUTCOME

Among the four fundamental plaque features, only spotty calcification, napkin-ring sign, and low attenuation were correlated with the primary outcome, but positive remodeling was not. The HRs increased in proportion to

ISSN:0975-3583,0976-2833 VOL12,ISSUE04,2021

the rise in the overall number of distinct plaque features. If two or more distinct characteristics are present, the plaque is considered a high-risk plaque [94].

8. CONCLUSION

In the modern era, coronary artery disease is the principal cause of mortality. MDCT examination of coronary artery disease is a promising non-invasive technique for assessment and plaque characterization. It shares in the generation of recommendations of management for better outcomes and prognosis.

9. REFERENCES

[1] Brevoord D, et al. Remote ischaemic conditioning to protect against ischaemia reperfusion injury: a systematic review and meta-analysis. PLoSOne2012;7:e42179. https://doi.org/10.1371/journal.pone.0042179.

[2] Libby P, Theroux P. Pathophysiology of coronary artery disease. Circulation .2005; 111: 3481-3488.

[3] Falk E, et al. Coronary plaque disruption. Circulation1995; 92: 657-671. https://doi.org/10.1161/01.CIR.92.3.657.

[4] Moreno PR, et al. Promoting mechanisms of vascular health: circulating progenitorcells, angiogenesis, and reverse cholesterol transport. J Ann Coll Cardiol2009; 53: 2315-2323.https://doi.org/10.1016/j.jacc.2009.02.057.

[5] Schaar JA, et al. Terminology for high risk and vulnerable coronary arteryplaques. Report of a meeting on the vulnerable plaque. June 17 and 18, 2003,Santorini, Greece. Eur Heart J 2004; 25: 1077-1082.https://doi: 10.1016/j.ehj.2004.01.002.

[6] Naghavi M, et al. From vulnerable plaque to vulnerable patient: a call for newdefinitions and risk assessment strategies: Part I. Circulation 2003; 108:1664-1672.doi: 10.1161/01.CIR.0000087480.94275.97.

[7] Muller JE, et al. Circadian variation in the frequency of onset of acute myocardialinfarction. N Eng J Med 1985; 313: 1315-1322.doi: 10.1056/NEJM198511213132103.

[8] Rosa GM,BaucknehtM,Mach F et al. The vulnerable coronary plaque: Update on imaging technologies. Thrombosis and Haemostasis 110[3].2013.1-17. DOI: 10.1160/TH13-02-0121 ·

[9] Lloyd-Jones D, Adams RJ, Brown TM, et al. American Heart Association Statistics Committee and Stroke Statistics Subcommittee. Heart disease and stroke statistics, 2010 update: a report from the American Heart Association. Circulation 2010; 121:e46–e215.doi: 10.1161/CIRCULATIONAHA.109.192667.

[10] Kolodgie FD, Burke AP, Farb A, et al. The thincap fibroatheroma: a type of vulnerable plaque: the major precursor lesion to acute coronary syndromes. CurrOpinCardiol 2001; 16:285–292.doi: 10.1097/00001573-200109000-00006.

[11] Virmani R, Kolodgie FD, Burke AP, Farb A, Schwartz SM. Lessons from sudden coronary death: a comprehensive morphological classification scheme for atherosclerotic lesions. ArteriosclerThrombVascBiol . 2000; 20:1262–1275. https://doi.org/10.1161/01.ATV.20.5.1262

[12] Saremi F and Achenbach S. Coronary Plaque Characterization Using CT. Cardiopulmonary Imaging.2014.DOI:10.2214/AJR.14.13760.

[13] Alsheikh-Ali AA, et al. The vulnerable atherosclerotic plaque: scope of the literature.Ann Intern Med 2010; 153: 387-395. https://doi.org/10.7326/0003-4819-153-6-201009210-00272.

[14] Burke AP, Virmani R, Galis Z, Haudenschild CC, Muller JE. 34th Bethesda Conference: task force 2—what is the pathologic basis for new atherosclerosis imaging techniques? J Am Coll Cardiol 2003; 41:1874–1886.

ISSN:0975-3583,0976-2833 VOL12,ISSUE04,2021

[15] Ohayon J, Finet G, Gharib AM, et al. Necrotic core thickness and positive arterial remodeling index: emergent biomechanical factors for evaluating the risk of plaque rupture. Am J Physiol Heart Circ Physiol2008;295:H717–H727. https://doi.org/10.1152/ajpheart.00005.2008

[16] De Korte CL, et al. Vascular ultrasound for atherosclerosis imaging. InterfaceFocus 2011; 1: 565-575.https://dx.doi.org/10.1098%2Frsfs.2011.0024

[17] Nissen SE, Yock P. Intravascular ultrasound: novel pathophysiological insights and current clinical applications. Circulation 2001; 103: 604-616.

[18] Rodriguez-Granillo GA, , Eugène P. Mc Fadden, Jiro Aoki, Carlos A. G. van Mieghem, Evelyn Regar, Nico Bruining & Patrick W. Serruyset al. In vivo variability in quantitative coronary ultrasound and tissue characterisation measurements with mechanical and phased array catheters. Int J Cardiovasc Imaging. 2006; 22: 47-53.

[19] Goar FG, et al. Intravascular ultrasound imaging of angiographically normalcoronary arteries: an in vivo comparison with quantitative angiography. J Am Coll Cardiol 1991; 18: 952-958.https://doi.org/10.1016/0735-1097[91]90753-v.

[20] Layland J, et al. Virtual Histology: A Window to the Heart of Atherosclerosis.Heart Lung Circ 2011; 20: 615-621.https://doi.org/10.1016/j.hlc.2010.12.002.

[21] Kume T, et al. Assessment of coronary arterial thrombus by optical coherencetomography. Am J Cardiol 2006; 97: 1713-1717.https://doi.org/10.1016/j.amjcard.2006.01.031

[22] Low AF, et al. In vivo characterisation of coronary plaques with conventionalgrey-scale intravascular ultrasound: correlation with optical coherence tomography.EuroIntervention 2009; 4: 626-632.https://doi.org/10.4244/eijv4i5a105

[23] Nair A, et al. Coronary plaque classification with intravascular ultrasoundradiofrequency data analysis. Circulation 2002; 106: 2200-2206.https://doi.org/10.1161/01.cir.0000035654.18341.5e

[24] Virmani R, et al. Pathology of the vulnerable plaque. J Am Coll Cardiol 2006;47: C13-C18. https://doi.org/10.1016/j.jacc.2005.10.065

[25] Nair ACD, Vince DG. Regularized autoregressive analysis of intravascular ultrasound data: improvement in spatial accuracy of plaque tissue maps. IEEE Trans UltrasonFerroelectr Freq Control 2004; 51: 420-431.https://doi.org/10.1109/tuffc.2004.1295427.

[26] Liang Y, et al. Measurement of 3D arterial wall strain tensor using intravascular B-mode ultrasound images: a feasibility study. Phys Med Biol .2010; 55:6377-6394.https://doi.org/10.1088/0031-9155/55/21/003.

[27] Prati F, et al. Expert review document on methodology, terminology, and clinical applications of optical coherence tomography: physical principles, methodology of image acquisition, and clinical application for Assessment of coronary arteries and atherosclerosis. Eur Heart J 2010; 31: 401-415.https://doi.org/10.1093/eurheartj/ehp433.

[28] Kitabata H, et al. Relation of microchannel structure identified by optical coherence tomography to plaque vulnerability in patients with coronary artery disease. Am J Cardiol 2010; 105: 1673-1678.https://doi.org/10.1016/j.amjcard.2010.01.346.

[29] Sandfort V, Lima L and Bluemke Da. Non-invasive Imaging of Atherosclerotic Plaque Progression: Status of Coronary CT Angiography. Circ Cardiovasc Imaging. 2015 July ; 8[7].

[30] Yuan C, et al. Carotid atherosclerotic plaque: non invasive MR characterization and identification of vulnerable lesions. Radiology 2001; 221: 285-299.https://doi.org/10.1148/radiol.2212001612.

ISSN:0975-3583,0976-2833 VOL12,ISSUE04,2021

[31] Takaya N, et al. Association between carotid plaque characteristics and subsequent ischaemic cerebrovascular: a prospective assessment with MRI-initial results. Stroke 2006; 37: 818-823.https://doi.org/10.1161/01.str.0000204638.91099.91.

[32] Sadat U, et al. High resolution magnetic resonance imaging-based biochemical stress analysis of carotid atheroma: a comparison of single transient ischaemic attack, recurrent transient ischaemic attacks, non-disabling stroke and asymptomatic patients group .Eur J VascEndovascSurg2011; 41: 83-90.https://doi.org/10.1016/j.ejvs.2010.09.006.

[33] Wasserman BA, et al. Carotid artery atherosclerosis in vivo morphologic characterization with gadolinium/enhanced double oblique MR imaging /initial results. Radiology 2002; 223: 566-573.https://doi.org/10.1148/radiol.2232010659.

[34] Achenbach S, et al. detection of coronary artery stenoses by contrast-enhanced, retrospectively electrocardiographically gated, multislice spiral computed tomography.Circulation 2001; 103: 2535-2538.https://doi.org/10.1161/01.cir.103.21.2535.

[35] Schroeder S, et al. Cardiac computed tomography: indications, applications, limitations and training requirements. Eur Heart J 2008; 29: 531-536.https://doi.org/10.1093/eurheartj/ehm544.

[36] Ehara S, et al. Spotty calcification typifies the culprit plaque in patients with acute myocardial infarction: an intravascular ultrasound study. Circulation 2004; 110: 3424-3429.https://doi.org/10.1161/01.cir.0000148131.41425.e9.

[37] Pundziute G, et al. Head-to-head comparison of coronary plaque evaluation between multislice and intravascular ultrasound radiofrequency data analisis. JACC Cardiovasc Imaging 2008: 1: 176-182.https://doi.org/10.1016/j.jcin.2008.01.007.

[38] Camici PG, et al. Non-invasive anatomic and functional imaging of vascular inflammation and unstable plaque. Eur Heart J 2012; 33: 1309-1317.https://doi.org/10.1093/eurheartj/ehs067.

[39] Motoyama S, et al. Multislice computed tomographic characteristics of coronary lesions in acute coronary syndromes. J Am Coll Cardiol 2007; 50: 319-326.https://doi.org/10.1016/j.jacc.2007.03.044.

[40] Maurovich-Horvat P, et al. The napkin-ring sign: CT signature of high-risk coronary plaques? JACC Cardiovasc Imaging 2010; 3: 440-444.https://doi.org/10.1016/j.jcmg.2010.02.003.

[41] Pflederer T, et al. Characterisation of culprit lesions in acute coronary syndromes using coronary dual-source CT angiography. Atherosclerosis 2010; 211:437-444.https://doi.org/10.1016/j.atherosclerosis.2010.02.001.

[42] Hyafil F, et al. quantification of inflammation with rabbit atherosclerotic plaques using the macrophage–specific CT Contrast agent N1177: a comparison with 18FDG PET/CT and histology. J Nucl Med 2009; 50: 959-965. DOI: 10.2967/jnumed.108.060749.

[43] Ropers D, Baum U, Pohle K, et al. detection of coronary artery stenoses with thin-slice multi-detector row spiral computed tomography and multiplanar reconstruction. Circulation 2003;107:664–6.https://doi.org/10.1161/01.cir.0000055738.31551.a9

[44] Ferencik M, Moselewski F, Ropers D, et al. Quantitative parameters of image quality in multi-detector spiral computed tomographic coronary imaging with submillimeter collimation. Am J Cardiol2003;92:1257–62.https://doi.org/10.1016/j.amjcard.2003.08.003.

[45] Austen WG, Edwards JE, Frye RL, et al. A reporting system on patients evaluated for coronary artery disease. Report of the Ad Hoc Committee for Grading of Coronary Artery Disease, Council on Cardiovascular Surgery, American Heart Association. Circulation 1975;51:5–40.https://doi.org/10.1161/01.cir.51.4.5.

[46] Achenbach S, Moselewski F, Ropers D, et al. detection of calcified and non-calcified coronary atherosclerotic plaque by contrast-enhanced, submillimeter multi-detector spiral computed tomography: a

ISSN:0975-3583,0976-2833 VOL12,ISSUE04,2021

segmentbased comparison with intravascular ultrasound. Circulation 2004;109:14–7.https://doi.org/10.1161/01.cir.0000111517.69230.0f.

[47] Hoffmann U, MoselewskiF , Nieman K etal. Non-invasive Assessment of Plaque Morphology and Composition in Culprit and Stable Lesions in Acute Coronary Syndrome and Stable Lesions in Stable Angina by Multidetector Computed Tomography. Journal of the American College of Cardiology. 2006.Vol. 47, No. 8.doi:10.1016/j.jacc.2006.01.041.

[48] Raff GL, Abidov A, Achenbach S, et al. SCCT guidelines for the interpretation and reporting of coronary computed tomographic angiography. J Cardiovasc ComputTomogr2009;3:122-36.https://doi.org/10.1016/j.jcct.2009.01.001.

[49] Hadamitzky M, Achenbach S, Al-Mallah M, et al. Optimized prognostic score for coronary computed tomographic angiography: results from the CONFIRM registry [COronary CT Angiography EvaluatioNFor Clinical Outcomes: An InteRnationalMulticenter Registry]. J Am Coll Cardiol2013;62:468-76.https://doi.org/10.1016/j.jacc.2013.04.064.

[50] Narula, J. et al. Arithmetic of vulnerable plaques for non-invasive imaging. Nat. Clin. Pract. Cardiovasc. Med. 5 [Suppl. 2].2008. S2–S10.https://doi.org/10.1038/ncpcardio1247.

[51] Pohle, K. et al. Characterization of non-calcified coronary atherosclerotic plaque by multi-detector row CT: comparison to IVUS. Atherosclerosis.2007. 190, 174–180.https://doi.org/10.1016/j.atherosclerosis.2006.01.013.

[52] Voros, S. et al. Prospective validation of standardized, 3-dimensional, quantitative coronary computed tomographic plaque measurements using radiofrequency backscatter intravascular ultrasound as reference standard in intermediate coronary arterial lesions: results from the ATLANTA [Assessment of tissue characteristics, lesion morphology, and hemodynamics by angiography with fractional flow reserve, intravascular ultrasound and virtual histology, and non-invasive computed tomography in atherosclerotic plaques] I study. JACC Cardiovasc. 2011. Interv. 4,198–208.https://doi.org/10.1016/j.jcin.2010.10.008.

[53] Achenbach, S. et al. CV Imaging: What was new in 2012? JACC Cardiovasc. 2013. Imaging 6, 714–734.https://doi.org/10.1016/j.jcmg.2013.04.005.

[54] Boogers, M. J. et al. Automated quantification of coronary plaque with computed tomography:comparison with intravascular ultrasound using a dedicated registration algorithm for fusion-based quantification. Eur. Heart J. 2012. 33, 1007–1016.https://doi.org/10.1093/eurheartj/ehr465.

[55] Dey, D. et al. Automated three-dimensional quantification of non-calcified coronary plaque from coronary CT angiography: comparison with intravascular US. 2010. Radiology 257, 516–522.https://doi.org/10.1148/radiol.10100681.

[56] Ozaki, Y. et al. Coronary CT angiographic characteristics of culprit lesions in acute coronary syndromes not related to plaque rupture as defined by optical coherence tomography and angioscopy. Eur. Heart J. 2011. 32, 2814–2823.https://doi.org/10.1093/eurheartj/ehr189.

[57] Pflederer, T. et al. Characterization of culprit lesions in acute coronary syndromes using coronary dual-source CT angiography.Atherosclerosis.2010.211, 437–444.https://doi.org/10.1016/j.atherosclerosis.2010.02.001.

[58] Ito T, et al. comparison of in vivo assessment of vulnerable plaque by 64-slice multislice computed tomography versus optical coherence tomography. Am. J. Cardiol. 2011. 107, 1270–1277. https://doi.org/10.1016/j.amjcard.2010.12.036.

[59] Kodama T., Kondo T., Oida A., Fujimoto S. & Narula, J. Computed tomographic angiography verified plaque characteristics and slow-flow phenomenon during percutaneous coronary intervention. JACC Cardiovasc. 2012. Interv. 5, 636–643.https://doi.org/10.1016/j.jcin.2012.02.016.

[60] Maurovich-Horvat, P. et al. The napkin-ring sign: CT signature of high risk coronary plaques? JACC Cardiovasc .Imaging.2010. 3, 440–444.https://doi.org/10.1016/j.jcmg.2010.02.003.

ISSN:0975-3583,0976-2833 VOL12,ISSUE04,2021

[61] Maurovich-Horvat, P. et al. The napkin-ring sign indicates advanced atherosclerotic lesions in coronary CT angiography. JACC Cardiovasc.. Imaging.2012. 5, 1243–1252.https://doi.org/10.1016/j.jcmg.2012.03.019.

[62] Yamamoto, H., Kitagawa, T. &Kihara, Y. Dose napkin-ring sign suggest possibility to identify rupture-prone plaque in coronary computed tomography angiography? J. Cardiol. 2013. 62, 328–329.https://doi.org/10.1016/j.jjcc.2013.02.020.

[63] Maurovich-Horvat PM, Ferencik M, Voros S, et al. Comprehensive plaque assessment by coronary CT angiography. Nat. Rev. Cardiol. advance online publication 22 April 2014.doi:10.1038/nrcardio.2014.60.

[64] Voros, S. et al. Coronary atherosclerosis imaging by coronary CT angiography: current status, correlation with intravascular interrogation and meta-analysis. JACC Cardiovasc. Imaging 2011. 4,537–548.https://doi.org/10.1016/j.jcmg.2011.03.006.

[65] Achenbach S. et al. Assessment of coronary remodeling in stenotic and nonstenotic coronary atherosclerotic lesions by multi-detector spiral computed tomography. J. Am. Coll. Cardiol. 2004. 43,842–847.https://doi.org/10.1016/j.jacc.2003.09.053.

[66] Gauss S. et al. Assessment of coronary artery remodelling by dual-source CT: a head-to-head comparison with intravascular ultrasound. Heart. 2011 97, 991–997.https://doi.org/10.1136/hrt.2011.223024.

[67] Mint z, G. S. et al. American College of Cardiology clinical expert consensus document on standards for acquisition, measurement and reporting of intravascular ultrasound studies [IVUS]. A report of the American College of Cardiology Task Force on clinical expert consensus documents. J. Am. Coll. Cardiol. 2001. 37,1478–1492.https://doi.org/10.1016/s0735-1097[01]01175-5.Mintz GS, Nissen SE, Anderson WD, Bailey SR, Erbel R, Fitzgerald PJ, Pinto FJ, Rosenfield K, Siegel RJ, Tuzcu EM, Yock PG.

[68] Kröner, E. S. et al. Positive remodeling on coronary computed tomography as a marker for plaque vulnerability on virtual histology intravascular ultrasound. Am. J. Cardiol. 2011.107,1725–1729.https://doi.org/10.1016/j.amjcard.2011.02.337.

[69] Taylor, A. J. et al. Coronary calcium independently predicts incident premature coronary heart disease over measured cardiovascular risk factors: mean three-year outcomes in the Prospective Army Coronary Calcium [PACC] project. J. Am. Coll. Cardiol. 2005. 46, 807–814.https://doi.org/10.1016/j.jacc.2005.05.049.

[70] Ferencik, M. et al. A computed tomography based coronary lesion score to predict acute coronary syndrome among patients with acute chest pain and significant coronary stenosis on coronary computed tomographic angiogram. Am.J. Cardiol. 2012. 110, 183–189.https://doi.org/10.1016/j.amjcard.2012.02.066.

[71] Motoyama, S. et al. Multislice computed tomographic characteristics of coronary lesions in acute coronary syndromes. J. Am. Coll. Cardiol. 2007. 50, 319–326.https://doi.org/10.1016/j.jacc.2007.03.044.

[72] Van Velzen, J. E. et al. Comprehensive assessment of spotty calcifications on computed tomography angiography: comparison to plaque characteristics on intravascular ultrasound with radiofrequency backscatter analysis. J. Nucl. Cardiol. 2011. 18, 893–903.https://doi.org/10.1007/s12350-011-9428-2.

[73] Joshi, N. V. et al. 18F-fluoride positron emission tomography for identification of ruptured and high-risk coronary atherosclerotic plaques: a prospective clinical trial. 2014. Lancet 383, 705–713.https://doi.org/10.1016/s0140-6736[13]61754-7.

[74] Taylor, C. A., Fonte, T. A. & Min, J. K. Computational fluid dynamics applied to cardiac computed tomography for non-invasive quantification of fractional flow reserve: scientific basis. J. Am. Coll. Cardiol. 2013. 61, 2233–2241.

ISSN:0975-3583,0976-2833 VOL12,ISSUE04,2021

[75] Nieman, K. & de Feijter, P. J. Aerodynamics in cardiac CT. Circ. Cardiovasc. Imaging. 2013. 6, 853–854.

[76] Slager, C. J. et al. The role of shear stress in the generation of rupture-prone vulnerable plaques.Nat. Clin. Pract Cardiovasc. Med. 2005. 2, 401–407.https://doi.org/10.1038/ncpcardio0274.

[77] Chatzizisis, Y. S. et al. Role of endothelial shear stress in the natural history of coronary atherosclerosis and vascular remodeling: molecular, cellular, and vascular behavior. J. Am.Coll. Cardiol. 2007. 49, 2379–2393.https://doi.org/10.1016/j.jacc.2007.02.059.

[78] Wentzel, J. J. et al. Endothelial shear stress in the evolution of coronary atherosclerotic plaque and vascular remodelling: current understanding and remaining questions. Cardiovasc. Res.2012. 96, 234–243.https://doi.org/10.1093/cvr/cvs217.

[79] Samady, H. et al. Coronary artery wall shear stress is associated with progression and transformation of atherosclerotic plaque and arterial remodeling in patients with coronary artery disease. Circulation .2011. 124, 779–788.https://doi.org/10.1161/circulationaha.111.021824.

[80] Gijsen, F. J. et al. 3D reconstruction techniques of human coronary bifurcations for shear stress computations. J. Biomech.2014. 47, 39–43.https://doi.org/10.1016/j.jbiomech.2013.10.021.

[81] Finn, A. V., Nakano, M., Narula, J., Kolodgie, F. D. &Virmani, R. Concept of vulnerable/unstable plaque. Arterioscler. Thromb. Vasc. Biol. 2010. 30, 1282–1292.

[82] Narula, J. et al . Histopathologic characteristics of atherosclerotic coronary disease and implications of the findings for the invasive and non-invasive detection of vulnerable plaques. J. Am. Coll. Cardiol. 2013. 61, 1041–1051.https://doi.org/10.1016/j.jacc.2012.10.054.

[83] Shmilovich, H. et al. Vulnerable plaque features on coronary CT angiography as markers of inducible regional myocardial hypoperfusion from severe coronary artery stenoses.Atherosclerosis.2011. 219, 588–595.https://doi.org/10.1016/j.atherosclerosis.2011.07.128.

[84] Min, J. K. et al. Diagnostic accuracy of fractional flow reserve from anatomic CT angiography. JAMA .2012.308, 1237–1245.https://doi.org/10.1001/2012.jama.11274.

[85] Kim, K. H. et al. A novel non-invasive technology for treatment planning using virtual coronary stenting and computed tomography derived computed fractional flow reserve.JACC Cardiovasc. Interv. 2014. 7, 72–78.https://doi.org/10.1016/j.jcin.2013.05.024.

[86] Li P, Gai LY, Yang X, Sun ZJ, JinQH . Computed tomography angiography guided percutaneous coronary intervention in chronic total occlusion. J Zhejiang UnivSci .B. 2011. 11: 568-574.

[87] Hsu JT, Kyo E, Chu CM, Tsuji T, Watanabe S . Impact of calcification length ratio on the intervention for chronic total occlusions. Int J Cardiol. 2011 150: 135-141.

[88] Von Ballmoos MW, Haring B, Juillerat P, AlkadhiH . Meta-analysis: diagnostic performance of low-radiation-dose coronary computed tomography angiography. Ann Intern Med . 2011. 154: 413-420.

[89] Ayad S W, Sobhy M A,El-sharkawy E M et al. Role of plaque characterization by 64-slice multi detector computed tomography in prediction of complexity of percutaneous coronary interventions. Journal of integrative cardiology.2015.vol1[5]:118-123.doi: 10.15761/JIC.1000132.

[90] Stone, G. W. et al. A prospective natural-history study of coronary atherosclerosis. N. Engl. J.Med. 2011. 364, 226–235.https://doi.org/10.1056/nejmoa1002358.

[91] Klass, O. et al. Coronary plaque imaging with 256-slice multi-detector computed tomography: interobserver variability of volumetric lesion parameters with semiautomatic plaque analysis software. Int. J. Cardiovasc. Imaging .2010. 26, 711–720.https://doi.org/10.1007/s10554-010-9614-3.

ISSN:0975-3583,0976-2833 VOL12,ISSUE04,2021

[92] Schepis, T. et al. Quantification of non-calcified coronary atherosclerotic plaques with dualsource computed tomography: comparison with intravascular ultrasound. Heart 96, .2010 .610–615.https://doi.org/10.1136/hrt.2009.184226.

[93] Kolossvary M, Szilveszter,Merkely B ,et al. Plaque imaging with CT—a comprehensive review on coronary CT angiography based risk assessment. Cardiovasc Diagn Ther 2017;7[5]:489-506.doi: 10.21037/cdt.2016.11.06.

[94] Yamamoto H,KiharaY,Kitagawa T et al. Coronary plaque characteristics in computed tomography and 2-year outcomes: The PREDICT study. Journal of Cardiovascular Computed Tomography. 2018. VOLUME12,ISSUE5, P436-443.:https://doi.org/10.1016/j.jcct.2018.07.001